Korean J. Chem. Eng., 40(5), 1077-1085 (2023)
DOI: 10.1007/s11814-022-1345-3

pISSN: 0256-1115
eISSN: 1975-7220

Detoxification of groundwater contaminated with Cr(VI) using continuous electrochemical cell equipped with copper foam electrode modified with palladium nanoparticles

Maedeh Alipour Kanafi, Majid Baghdadi†, and Naser Mehrdadi

School of Environment, College of Engineering, University of Tehran, P. O. Box: 1417853111, Tehran, Iran
(*Received 13 May 2022 • Revised 1 November 2022 • Accepted 10 November 2022*)

Abstract−This study investigated the detoxification of water contaminated with hexavalent chromium through a catalytic electrochemical reduction process using metallic foam cathodes. To select the proper materials to be used in a continuous electrochemical cell, batch experiments were performed on copper and nickel metallic foams, as potential cathodes, in the presence and absence of a coating layer of either palladium or silver nanoparticles, as potential catalysts. Regarding the results, copper foam and copper foam coated with palladium nanoparticles (PdNPs) were chosen. Next, the effects of parameters including pH, flow rate, electrical current intensity, and the initial concentration of hexavalent chromium were studied utilizing the continuous column of copper foam before and after adding PdNPs. The response surface methodology and the Box-Behnken Design approach were applied to optimize the significant parameters. Results indicated that the palladium nanocatalyst has significant effects on reduction efficiency. Through further experiments, we also found that the presence of nitrate and other coexisting ions has negligible impact on reduction efficiency. The optimum charts of chromium reduction were plotted based on the results. A sample optimum point gives a 97.8% reduction efficiency at pH=7, flow rate=50 mL min^{-1}, initial concentration=0.45 mg L^{-1}, and electric current of 0.3 A.

Keywords: Hexavalent Chromium, Electrochemical Reduction, Palladium Nanoparticles, Contaminated Water, Metal Foam

INTRODUCTION

According to the World Economic Forum (WEF), the water crisis is one of the most serious challenges regarding natural resources all over the world [1]. In this regard, heavy metals are known as one of the most important aquatic contaminants in terms of non-degradability and toxicity [2,3]. More than 70% of chromium and its compounds, which are considered among the most dangerous heavy metals, are released into the environment due to human activity and as a result of different industries, such as paint, leather tanning, textile, electroplating, and the processes related to metallurgy and protection of metal corrosion. On the other hand, small amounts of chromium exist in the rocks and soils naturally. Erosion and weathering of chromium-containing rocks is the main cause of the release of chromium into groundwater [4].

The chemical behavior and toxicity level of different forms of chromium are related to their oxidation number. Cr(III) and Cr(VI) are the most common forms of chromium in water. Cr(III) can easily deposit as a hydroxide or adsorb on the surface of solids, whereas Cr(VI) is highly soluble with a high degree of mobility [5]. Cr(VI), even at very low concentration, is very toxic and can be a hazard to the environment and human health due to its high toxicity and carcinogenicity [6-8]. Inhalation of a large amount of Cr(VI) can cause nasal ulceration, asthma, and skin contact can lead to skin allergies. Furthermore, exposure to this substance for long periods may cause liver failure, neurological disease, genetic mutations, and cancer. However, Cr(III) is 500 to 1,000 times less dangerous compared to Cr(VI) [9]. Although, the World Health Organization's (WHO) guidelines for drinking water quality still consider the maximum limit of 50 μg L^{-1} for total chromium in drinking water. However, during the last few years, some countries have started to introduce a limit of 10 μg L^{-1} for Cr(VI) [10-12].

Several methods have been proposed for removing Cr(VI) from contaminated water, including ion exchange [6,13], adsorption [14,15], membrane technology [8,16], biological methods [17,18], chemical reduction and precipitation [19], and electrochemical reduction [20]. One disadvantage of chemical methods is that they may introduce a high dose of chemicals into the water, and therefore add other contaminants to it, or they may lead to sludge formation, which can be difficult to be treated or disposed [19].

In an electrochemical system, an anode and a cathode act as acceptor and donor of electrons, respectively. In the electrochemical reduction of Cr(VI), electron exchange between the cathode and Cr(VI) leads to the transformation to Cr(III) without adding any chemicals to the water. On the other hand, easy maintenance and a low level of environmental hazard are among the main advantages of the electrochemical methods for removing Cr(VI). Therefore, this method is known as an environmentally clean process. In addition to the material used for the electrodes, other parameters that can influence the reduction process are the pH value, presence

†To whom correspondence should be addressed.
E-mail: m.baghdadi@ut.ac.ir

of coexisting species, flow rate, electrical current intensity, and the initial concentration of contaminant [14,21].

The selection of dimensions and materials of the cathode used in electrochemical cells is the most important point. Common materials used for the fabrication of cathodes include lead (Pb), tin (Sn), iron (Fe), copper (Cu), platinum (Pt), and titanium (Ti). Cathodes are manufactured in rod or plate shape conventionally. On the other hand, the active surface area, which plays a significant role in the reduction process, is limited in plate cathodes. Low surface area can decrease the reaction rate, thereby increasing reaction time [22,23]. Recently, metallic foams with a porous structure providing a high active surface area have attracted the attention of researchers [24, 25]. Therefore, it is expected that using metallic foams with a huge surface area improves the efficiency of contaminant removal and increases the reaction rate. Carbon-based materials, like graphite, are widely employed as the anode in the Cr(VI) electroreduction process because they are resistant to oxidation and, therefore, they act as an inert anode. In addition, graphite is not corroded, while iron anodes are dissolved during the reaction, producing iron hydroxide sludge [26-28].

Electroreduction methods based on metallic foams can be very efficient and more suitable compared to other methods for removing Cr(VI). In this method, very little electrical energy is used and power consumption is negligible. Immobilization of nanoparticles, such as palladium or silver nanoparticles, on the surface of metallic foam, can potentially increase the specific surface area and produce hydrogen radical, which is a strong reductant, thereby increasing the reduction efficiency and removal rate [29].

In summary, we studied the reduction efficiency of Cr(VI) by comparing the behavior of copper foam and nickel foam as cathodes and comparing the catalytic properties of palladium and silver nanoparticles coated on the surface of the cathode to determine the best combination. Then the possible effects of some parameters including pH, flow rate, current intensity, and initial dose of contaminant on the reduction efficiency were investigated. Moreover, removing Cr(VI) in the presence of nitrate and the other coexisting ions was examined.

MATERIALS AND METHODS

1. Materials

Copper foam (100×100×2 mm) and nickel foam (100×100×2 mm) with a porosity of 90 pores per inch (PPI) were provided from Latech (Singapore) and used as the cathode. Graphite plate (10×10×1.5 cm, Toray Industries, Inc.) and carbon fabric (Coarse, Unidirectional, Iran Composite shop) were used as the anode. The experiments related to the reduction of Cr(VI) were carried out using a power supply (Megatek MP-3010 DC, Taiwan) and a peristaltic pump (Sina Company). To coat the catalyst nanoparticles on the metallic foams, various salts including NH_4Cl, $PdCl_2$, and $AgNO_3$ were purchased from Merck (Darmstadt, Germany). For preparing a standard solution of Cr(VI) with a concentration of 1,000 mg L^{-1}, a certain amount of $K_2Cr_2O_7$ was dissolved in deionized water. Cr(VI) kit based on the 1, 5-diphenylcarbazide method was provided by Zist Tajzieh Gostar Co (Iran, Arak) and used for determining the amount of Cr(VI) remaining in the solution. For adjusting the initial pH of the solution, NaOH and HCl solutions (1 mol L^{-1}) were used. A buffer solution (pH=4) was prepared using solutions of acetic acid and sodium acetate (0.1 mol L^{-1}). All materials whose suppliers are not mentioned were provided by Merck Company.

Table 1. Analysis of groundwater sample

Cation	mg L^{-1}	Anion	mg L^{-1}		
Ca^{2+}	111	HCO_3^- (as $CaCO_3$)	171	TDS[a]	509 mg L^{-1}
K^+	1.5	Cl^-	62	EC[b]	719 μs cm^{-1}
Mg^{2+}	22	SO_4^{2-}	63	DO[c]	59 mg L^{-1}
Na^+	69	NO_3^-	67	pH	6.82
Fe	0.02				
Mn^{2+}	ND[d]				
Cr^{6+}	ND				

[a]Total dissolved solids, [b]Electrical conductivity, [c]Dissolved oxygen, [d]Not detected

2. Water Analysis

The composition of the groundwater used in this research is presented in Table 1. In addition, groundwater spiked with Cr(VI) was used to evaluate the efficiency of the process in the real groundwater matrix.

3. Preparation of Coated Cathodes

First, the surface of the metallic foam was washed with nitric acid (0.5% w/v) to remove metal oxides from the surface of the electrodes. For coating the surface of metallic foam with PdNPs, a solution containing 1.5 mM of $PdCl_2$ and 15 mM of NH_4Cl was prepared. Using hydrochloric acid (37%), the pH value of the coating solution was lowered to 1 [30]. To coat the cathode with silver nanoparticles, a solution containing 1.5 mM of $AgNO_3$ was prepared. A buffer solution containing 820 mL of acetic acid (0.1 mol L^{-1}) and 180 mL of sodium acetate (0.1 mol L^{-1}) was used to maintain the pH of the $AgNO_3$ solution at the level of 4 [25,31]. For each coating process, 500 mL of the initial solution was poured into a rectangular open container made of plexiglass with dimensions of 8×10×10 cm (L×W×H). In this container, the metallic foam cathode and the graphite plate anode are placed at a distance of 3 cm from each other. A magnetic mixer was used to stir the batch system. An adjustable digital DC power supply provided an electrical current of 20 mA between the electrodes for an hour to complete the coating process. Bare cathodes and different cathodes prepared through this coating process were used to compare their reduction efficiency. By comparing the results obtained from batch experiments, the most suitable cathode was selected. After that, the selected foam was used in a continuous electroreduction cell and coated with a suitable catalyst. For this purpose, two liters of the coating solution was pumped into the column under an upward flow using a peristaltic pump (10 $mLmin^{-1}$). This process was carried out for several cycles for two hours.

4. Characterization

The morphology of the bare copper foam and copper foam coated with PdNPs was studied using a TeScan-Mira III field-emission scanning electron microscopy (FESEM Czech Republic) to identify the presence of PdNPs on the surface of the copper bed and

measure the approximate size of PdNPs. EDAX analysis was used for detecting the type of elements and measuring the palladium content on the surface of the foam.

5. Analytical Methods

Hach-DR 5000 (Germany) spectrophotometer was used for determining the concentration of Cr(VI). The pH value of solutions was measured with a Swiss Metrohm 691 pH Meter. Inductively coupled plasma-optical emission spectroscopy (ICP-OES) (VISTA-PRO, Varian-Inc., USA) was used to determine the concentration of the Pd^{2+} in the coating solution after the coating process.

6. Fixed-bed Column Experiments

To investigate the effects of various parameters on the efficiency of Cr(VI) reduction and bring the experiments closer to practical conditions, a special reduction column was designed and built. For this purpose, a plexiglass cylindrical tube with an internal diameter of 26 mm, an outer diameter of 30 mm, and a length of 300 mm was used. Eight 7×10 cm^2 copper foam plates were attached to each other to form an integrated plate with a size of 28×20 cm^2 and used as the cathode in the reduction column. Carbon fabric (anode) with a length of 40 cm and copper foam (cathode) with a length of 28 cm were put together as two perfectly matching plates, and to prevent contact between the two plates, a porous plastic sheet was placed between them. Note that these three layers fit perfectly, and they can be considered as a single integrated plate. Using a multi-meter device ensured that there was no connection between the cathode and anode plates. Then, the integrated plate was wrapped around a plexiglass rod with a diameter of 1 mm. The wrapping of the plate around the rod continued until it eventually formed a cylindrical shape with a cross-section of concentric circles and with a diameter equal to the inner diameter of the plexiglass tube (Fig. 1(a)). Then, both ends of the tube were enclosed by circular plexiglass plates and sealed with a special type of glue. Three holes with diameters of 0.5, 0.5, and 0.9 mm were drilled in these circular plates to provide the required space for connecting the power supply to the cathode and anode plates and placing the water inlet/outlet, respectively. A section of the carbon fabric (anode) with a length of 5 cm was left out of the caps on both ends of the tube for connecting it to the power supply, and then the tube was sealed well. A few wire strands were placed on the inner wall of the column that extended through the designated holes at both ends of the column for connecting the metallic foam cathode to the power supply, and sealing was completed. Two pipes were attached to both ends of the column in their designated place to act as water inlet/outlet ports. Also, both ends of the anode and cathode plates were connected to the power supply so that the potential distribution would be uniform.

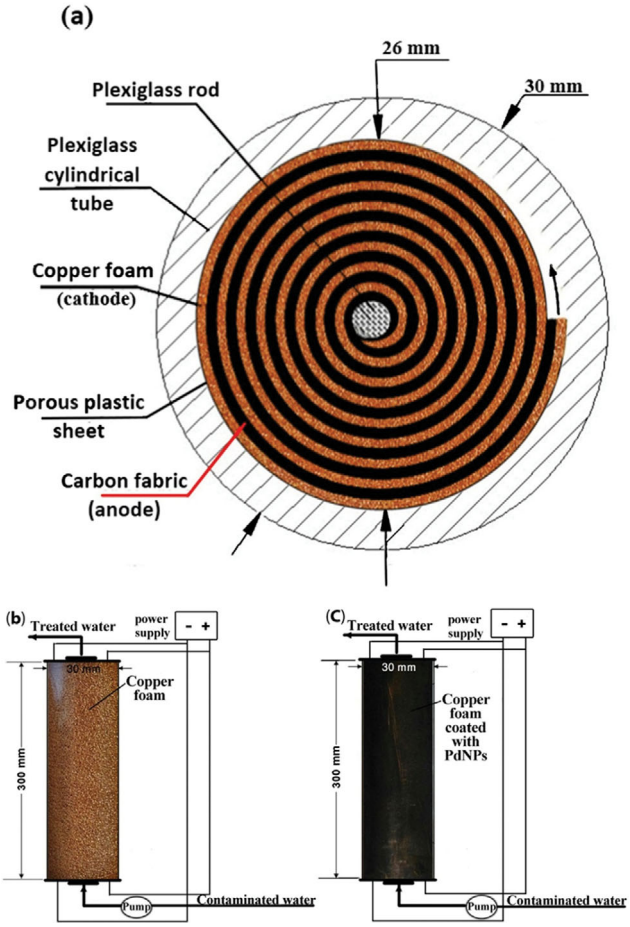

Fig. 1. (a) Cross-section of the special column built for the electrochemical reduction of Cr(VI) (b) Schematic diagram of the Cr(VI) reduction column with a cathode bed of copper foam and (c) Copper foam cathode coated with PdNPs.

To investigate the catalytic effects of PdNPs, a comparison was made between the reduction efficiency of Cr(VI) using bare copper foam and copper foam coated with PdNPs. For this purpose, the surface of the copper foam cathode in the reduction column was coated by the process described in the previous sections. The fixed-bed column, before and after coating the copper foam bed with PdNPs, is shown in Fig. 1(b) and c, respectively.

In this study, reduction column experiments were performed using copper foam cathode and copper foam cathode coated with PdNPs so that the experimental results would be more precise and

Table 2. Experimental range and levels of the independent variables

Variables	Factor	Unit	Copper foam cathode			Copper foam cathode coated with PdNPs		
			Levels			Levels		
			−1	0	+1	−1	0	+1
C	A	mg L^{-1}	0.1	0.3	0.5	0.1	0.45	0.8
pH	B	-	5	7	9	5	7	9
Q	C	$mLmin^{-1}$	10	30	50	20	50	80
I	D	A	0.1	0.3	0.5	0.1	0.3	0.5

comprehensive. Hence, to optimize the important parameters of the electroreduction cell composed of a copper foam and copper foam coated with PdNPs, two sets of experiments were designed by Design Expert 10 software using the response surface Box-Behnken method. The variable parameters of these experiments include the initial concentration of Cr(VI), the intensity of the applied current, flow rate, and pH value. Process optimization was performed based on the reduction efficiency (%R). Since four variables were chosen in each set of experiments, according to Eq. (1), 29 experiments were needed for each cathode [32].

$$N=2^n+2n+n_c=2^4+(2\times4)+5=29 \quad (1)$$

Five experiments were completely identical and repetitive so as to determine the level of error in experiments. The range of each variable is listed in Table 2, while the design matrix of experiments for copper foam cathode and copper foam coated with PdNPs is shown in Table S1.

7. Error Analysis

The residual root-mean-square error (RMSE) was used to evaluate the agreement between the experimental data and predictions using models. The related equation is as follows:

$$RMSE=\sqrt{\frac{1}{n-p}\sum_{i=1}^{n}\left(\frac{C_e}{C_0}\text{exp}-\frac{C_e}{C_0}\text{cal}\right)_i^2} \quad (2)$$

where $\frac{C_e}{C_0}$exp is the experimental results, $\frac{C_e}{C_0}$cal is the calculated values using the model, n is the number of experimental data, and p is the number of model parameters. RMSE should be as small as possible [33].

RESULTS AND DISCUSSION

1. Selection of Cathode and Catalyst

To select the most suitable material for metallic foam cathode (i.e., copper or nickel) and choose the proper catalyst for coating the surface of the cathode (i.e., palladium or silver), various experiments were carried out and the results were discussed. In these batch experiments, all the parameters, except the material used as the cathode and the catalyst, were kept constant. The experiments were carried out under an initial concentration of Cr(VI) equal to 0.2 mg L^{-1}, a current intensity of 0.1 A, and a pH value of 7. A mixer was used for providing uniform mass transfer. As shown in Fig. 2(a), the copper foam cathode coated with PdNPs had better performance and was able to reduce more chromium during one hour of running the experiment. The results showed that copper foam cathode coated with PdNPs had a distinguished performance as a cathode. As a consequence, the palladium coating had a significant impact on improving the reduction efficiency and reaction

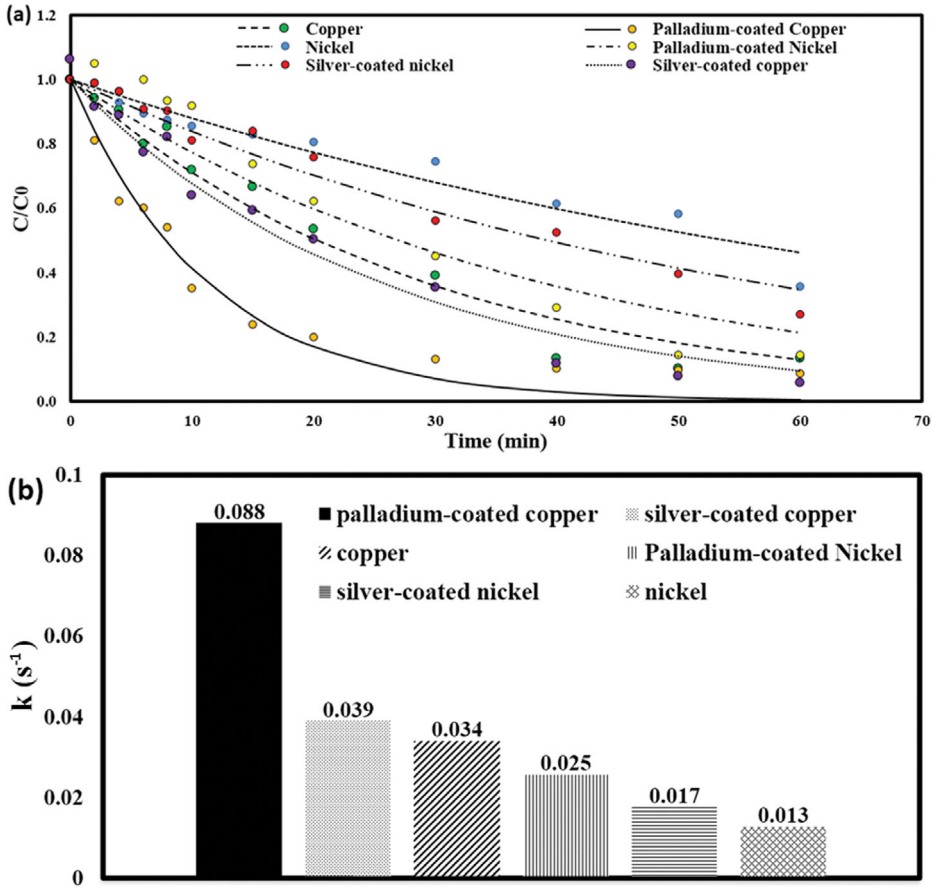

Fig. 2. The comparison of the (a) efficiency rates and (b) reaction constants (k) of removing Cr(VI) by using different materials as cathodes and coating them with different catalysts.

rates. The reaction rate constant per each material is demonstrated in Fig. 2(b). The higher the constant (k), the faster the reaction, and the higher the reduction efficiency for a given time. A simple comparison using the bar chart shows that the copper foam cathode coated with PdNPs had a reaction constant (k) three times greater than the copper foam and more than twice greater than the silver-coated copper foam. This higher reaction constant is due to the special properties of palladium in the adsorption of hydrogen molecules at its surface and converting it to hydrogen radical [30]. Based on these results, the copper foam coated with PdNPs was selected as the most suitable cathode for the preparation of the reduction column.

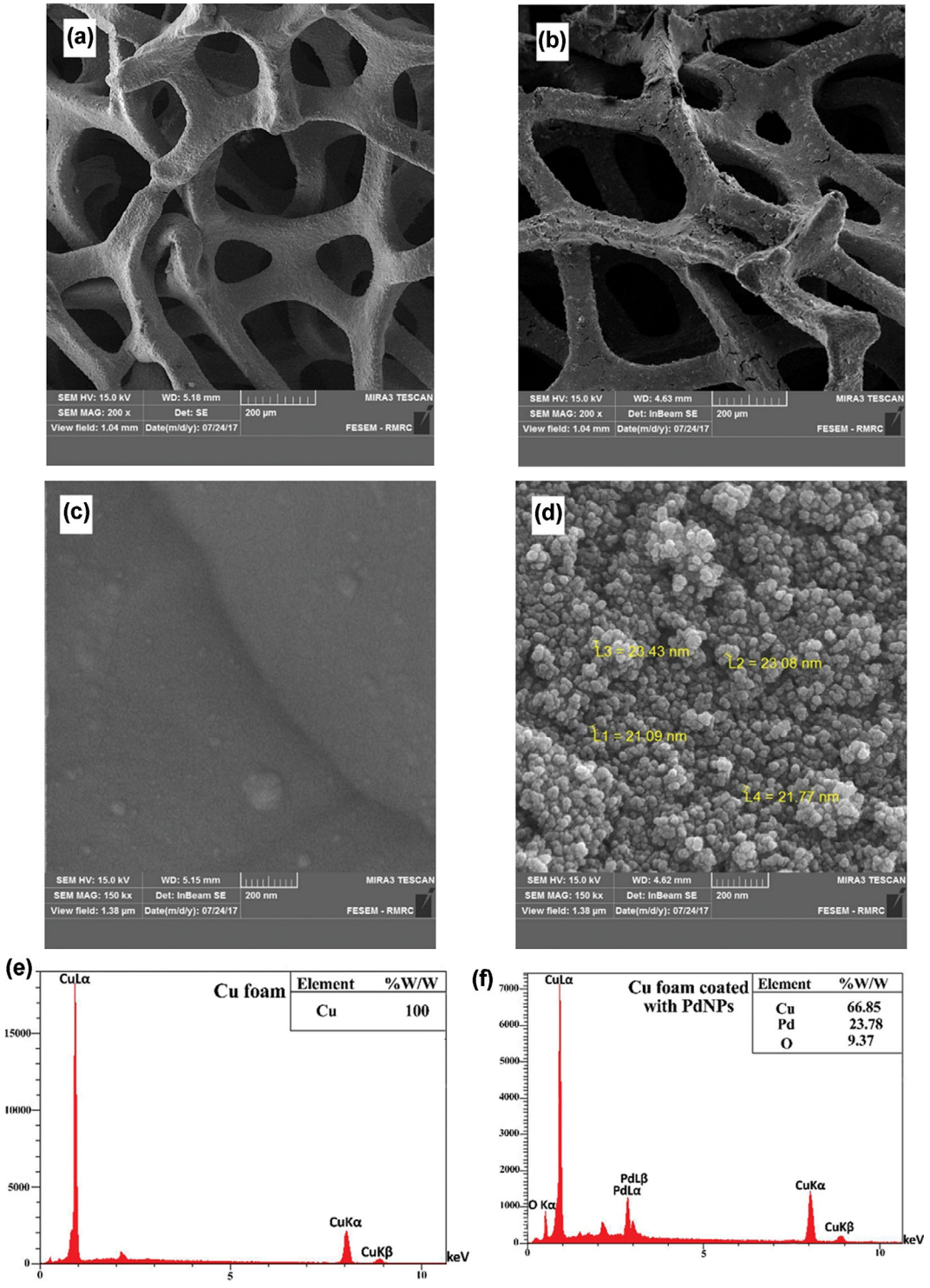

Fig. 3. FESEM images of copper foam at (a) 200 µm, (c) 200 nm, and copper foam coated with PdNPs at (b) 200 µm, (d) 200 nm, The EDS result for (e) copper foam and (f) for copper foam coated with PdNPs.

2. Morphological Study of the Surface of the Bare Copper Foam and Copper Foam Coated with PdNPs

Results of the FESEM analysis are presented in Fig. 3(a)-(c). These images show the surface of copper before and after coating with PdNPs. As can be seen, the coating process has been properly conducted and the surface of the copper foam is well-coated. Moreover, according to the study conducted by Li et al. [34] and also the results of this study, the surface of the copper foam coated with PdNPs is rougher than bare copper foam. The diameter of the PdNPs is shown in Fig. 3(d). The measured diameter of these nanoparticles approximately falls in the range of 21 to 23 nm. The results of the energy dispersive spectroscopy (EDS) analysis are presented in Fig. 3(e) and (f), which show the amount (W/W %) of each element in the sample.

3. Measuring the amount of Palladium Coated on the Surface of the Copper Foam Cathode

In line with Tabatabaei et al. [35] and based on the ICP results of this study, the concentration of PdNPs in the initial solution and the solution passed through the column with a copper bed was 169.05 and 4.32 mg L^{-1}, respectively. Therefore, 97.44% of Pd^{2+} content was coated on the copper foam. According to the nominal density of 0.03 g cm^{-2} for copper foam plates, the total surface area of eight foams (5.505 g) used in the column is 1,468 cm^2. Therefore, the amount of PdNPs that have coated the surface of the copper foam bed is equal to 0.1795 mg cm^{-2}. In fact, this clearly shows that even trace amounts of PdNPs can significantly improve the reduction efficiency of Cr(VI).

4. Statistical Analysis

Quadratic models for the reduction efficiency of Cr(VI) (Y) using the copper foam cathode and copper foam cathode coated with PdNPs are presented in Eqs. (3) and (4), respectively. The equations are formulated by Design Expert 10 software, which determines the reduction efficiency as a function of the initial concentration of Cr(VI) (A), pH value (B), the flow rate in the reduction column (C), and current intensity (D).

$$R\%=109.7638+92\times A-5.5556\times B-0.4354\times C+27.3582\times D-300\times A\times D-0.0687\times B\times C+21.4583\times B\times D+3.5625\times C\times D-0.0065\times C^2-279.162\times D^2 \quad (3)$$

$$R\%=39.7233+134.845\times A+3.97083\times B+2.51914\times C-87.0415\times D-17.25\times A\times B-1.58333\times A\times C+82.1429\times A\times D-0.205833\times B\times C+22.875\times B\times D+0.8875\times C\times D-0.0112705\times C^2-192.024\times D^2 \quad (4)$$

To determine the significance of the proposed model and investigate the contribution of each variable, analysis of variance (ANOVA) was performed. In this analysis, a small p-value (<0.05) indicates that the corresponding parameter is significant [32]. In the case of using the copper foam cathode, the p-values of parameters B, C, D, AD, BD, CB, C^2, and D^2 were less than 0.05, while for coated copper foam, all of the parameters except A^2 and B^2 had a p-value <0.05. Therefore, these parameters are considered significant in the model. For both cases, the p-value of the overall model is less than 0.0001, which indicates that the proposed model is significant and fits the data. For both cases, according to the p-value, lack-of-fits were not significant, which indicates that the data fit the proposed model well [36]. As can be seen in Table S2, the R^2 values of the models for both cathodes were very close to 1, indicating a strong correlation between the experimental results and the data predicted by the model [37]. Comparing the reduction efficiency of Cr(VI) using the experimental results and model predictions (Table S1) clearly shows that these values are strongly correlated. Therefore, the proposed model is valid for both cathodes, and the predicted reduction efficiencies are acceptable.

5. The Effects of Variables on the Reduction Efficiency

Using a perturbation plot, the influence of each parameter in a given point of design space can be evaluated and compared. In this plot, the higher slope of a curve indicates that the corresponding parameter has a greater influence on the removal efficiency. As can be seen in Fig. 4, increasing the current intensity resulted in higher reduction efficiency while increasing the other parameters had an adverse effect on the reduction efficiency. Fig. 4(a) shows that in the case of using the copper foam, two parameters, current intensity (D: I) and flow rate (C: Q), have the greatest influence on the reduction efficiency, respectively. Moreover, Fig. 4(b) shows that in the case of using the copper foam coated with PdNPs, the current intensity has a relatively higher influence, while other parameters are significant and influential.

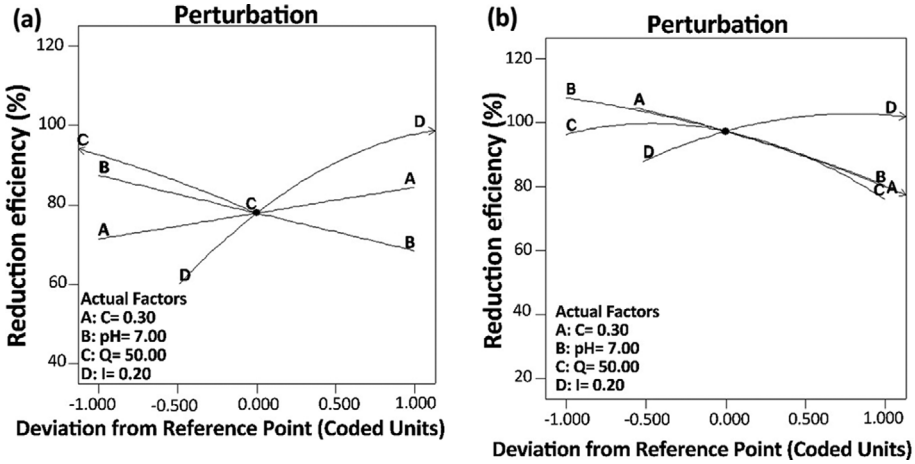

Fig. 4. Perturbation plots for Cr(VI) reduction by (a) Copper foam cathode and (b) PdNPs coated copper foa.

6. Effect of Independent Variables and their Interactions on the Reduction Efficiency

Fig. S1 shows the response surface plots for the case of using the copper foam cathode. Fig. S1(a) shows the response surface plot for two variables, current intensity and initial concentration, for pH=5 and a flow rate of 30 mLmin^{-1}. As can be seen, at the minimum level of initial concentration, reduction efficiency increases by increasing the current intensity. Fig. S1(b) also shows the response surface plot for two other variables, flow rate and current intensity, for pH=5 and an initial concentration of 0.1 mg L^{-1}. As can be seen, the maximum level of reduction efficiency was 100% and a complete reduction of Cr(VI) was achieved. Generally, increasing the current intensity resulted in a higher reduction efficiency. At the maximum and minimum levels of current intensity, different behaviors were observed with the increase in flow rate. At the maximum level of current intensity, increasing the flow rate increased the reduction efficiency. This behavior is probably caused by the increase of active sites due to the higher intensity of current and proper mass transfer due to the higher flow rates. Fig. S1(c) shows the relationship between pH value and the current intensity for the maximum level of flow rate (50 mL min^{-1}) and an initial concentration of 0.5 mg L^{-1}. Generally, increasing the pH value decreases the reduction efficiency, while increasing the current intensity will increase it.

Fig. S2 shows the response surface plots for the case of using the copper foam cathode coated with PdNPs. This figure includes the interaction of current intensity and initial concentration of Cr(VI) (Fig. S2(a)), the interaction of flow rate and current intensity (Fig. S2(b)), the interaction of flow rate and initial concentration (Fig. S2(c)), the interaction of pH value and initial concentration (Fig. S2(d)), the interaction of pH value and flow rate (Fig. S2(e)), and the interaction of pH value and current intensity (Fig. S2(f)). As can be seen, increasing the current intensity generally tends to increase the reduction efficiency, while increasing pH value, flow rate, and the initial concentration variables have adverse effects on the reduction efficiency.

In both cases, the copper foam and copper foam coated with PdNPs, as the flow rate and initial concentration of Cr(VI) increase, the reduction efficiency drops consequently. For instance, according to Eqs. (3) and (4), considering 0.3 mg L^{-1} of initial concentration of Cr(VI), pH of 7, 50 mL min^{-1} of flow rate, and 0.2 A of current intensity, reduction efficiency was 78.3% and 94.5% for copper foam and copper foam coated with PdNPs, respectively.

Table 3. The composition of stock solution of TDS with a concentration of 1,000 mg L^{-1}

Cation	mg L^{-1}	Anion	mg L^{-1}
Na^+	91.80	HCO_3^-	243.34
Ca^{2+}	137.66	Cl^-	243.92
Mg^{2+}	57.70	SO_4^{2-}	227.81

While other parameters were kept unchanged, by increasing the flow rate from 20 mL min^{-1} to 50 mL min^{-1}, reduction efficiency using both cathodes decreased and more decrease for copper foam was observed (5-15 percentage), which shows its higher sensitivity to flow rate. The results show that using the PdNPs catalyst, higher reduction efficiency was achieved.

7. Effect of Coexisting Ions

The potential effects of nitrate ions and total dissolved solids (TDS) on the reduction efficiency of Cr(VI) were studied separately using the copper foam cathode coated with PdNPs. Several solutions with different concentrations of nitrate ions (200, 150, 100, 50, and 25 mg L^{-1}) and TDS (1,000, 800, 400, 200, and 100 mg L^{-1}) were prepared using potassium nitrate and salts presented in Table 3, respectively. Similar conditions (I=0.3 A, Q=50 mL min^{-1}, Cr(VI)= 0.45 mg L^{-1}, pH=7, and sampling time of 30 min) were applied. The results are shown in Fig. 5(a) and (b). Although increasing the nitrate concentration diminishes the reduction efficiency, it can be ignored because of its low adverse effect. Furthermore, TDS had no significant effect on the reduction efficiency.

8. Optimization

Using Eq. (4), three plots (Fig. 6) were obtained for the initial concentrations of 0.1, 0.45, and 0.8 mg L^{-1}. Considering the limit of 0.01 mg L^{-1} for Cr(VI) in drinking water, the reduction efficiency of each plot is set in such a way that the remaining concentration of Cr(VI) in the treated water is less than 0.01 mg L^{-1}. The purpose of the optimal plots presented in this section is to provide a practical guide for selecting the parameters to reduce the Cr(VI) concentration to the acceptable limit. For instance, at pH=7 when the initial concentration is 0.45 mg L^{-1}, by setting the current intensity to at least 0.3 A, Cr(VI) concentration in treated water is less than 0.01 mg L^{-1} at the flow rates up to 50 mL min^{-1}.

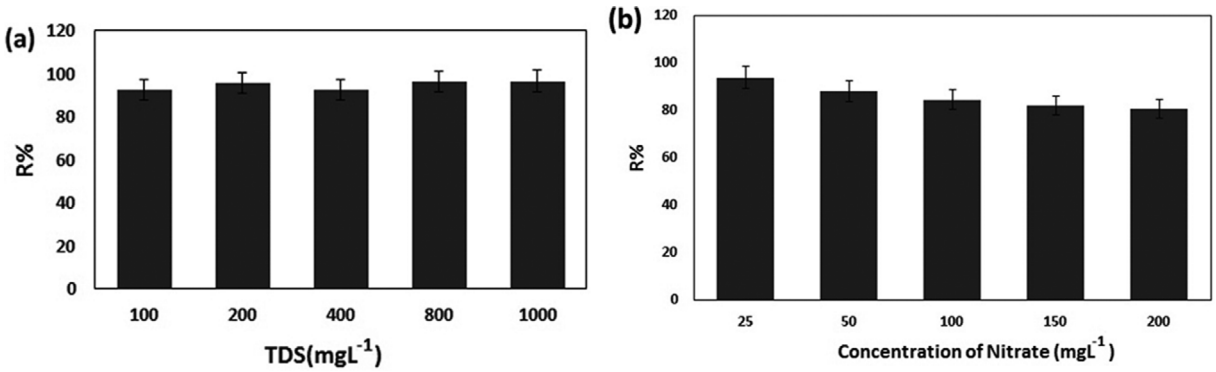

Fig. 5. Effect of (a) nitrate ions and (b) TDS on the reduction efficiency using copper foam coated with PdNPs.

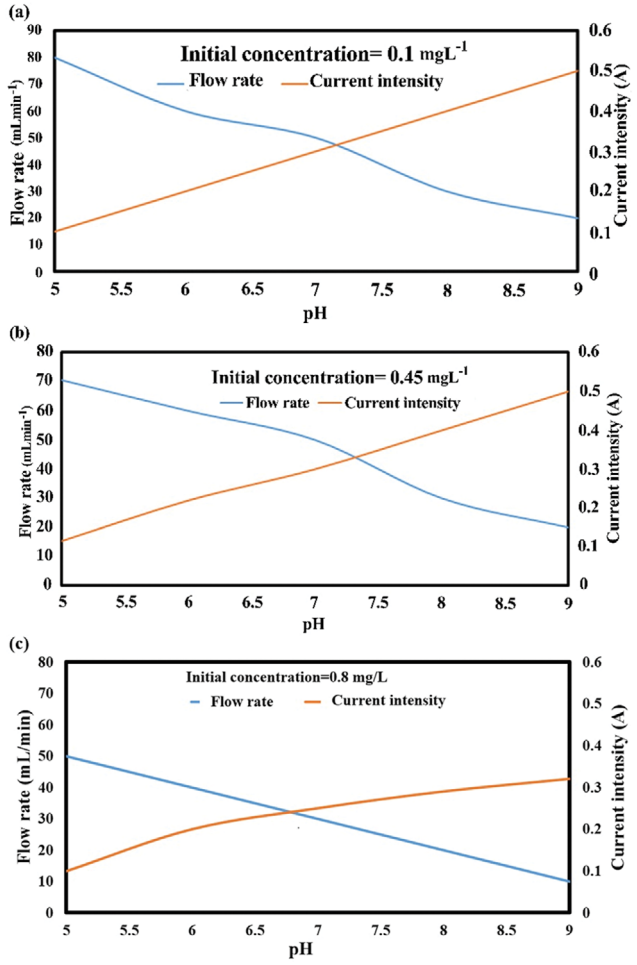

Fig. 6. Optimal plots of the experiment's variables for the initial concentration of Cr(VI) equal to (a) 0.1 mg L^{-1} (b) 0.45 mg L^{-1} (c) 0.8 mg L^{-1}.

9. Stability of PdNPs

According to Li et al. [34], to estimate the stability of the PdNPs on the cathode surface, ten sequence cycles of the experiment were run under the optimized condition of pH of 7, initial Cr(VI) concentration of 0.45 mg L^{-1}, the current intensity of 0.3 A, and flow rate of 50 mL min^{-1}. As shown in Fig. 7, an average reduction efficiency of 95.8% was obtained, indicating no significant decrease in the system performance. Therefore, it can be concluded that PdNPs were not detached from the surface of the cathode.

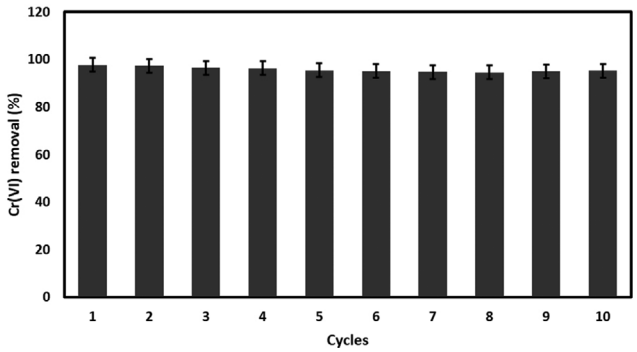

Fig. 7. Investigation of stability of PdNps on the reduction of Cr(VI) (pH: 7, initial concentration of Cr(VI): 0.45 mg L^{-1}, flow rate: 50 mL min^{-1}, and current intensity: 0.3 A).

10. Investigating the Reduction Mechanism

The mechanism of chromium reduction is either direct or indirect-catalytic reduction. In the case of direct reduction, Cr(VI) is reduced by receiving an electron from the cathode. In the case of indirect-catalytic reduction, palladium adsorbs the produced hydrogen gas and converts it to H^0, which is a strong reductant for the reduction of Cr(VI) [30,38]. In the electrolytic cell, several reactions occur at the cathode surface (Eqs. (5) and (6)). The reaction in the surface of the anode is presented in Eq. (7).

$$Cr_2O_7^{2-}+14H^++6e^-\rightarrow 2Cr^{3+}+7H_2O \quad (5)$$

$$2H_2O+2e^-\rightarrow H_2+2OH^- \quad (6)$$

$$2H_2O\rightarrow 4H^++O_2+4e^- \quad (7)$$

CONCLUSION

The reduction of Cr(VI) from contaminated water was investigated. Using graphite anode and copper and nickel foam cathodes (bare and coated with nanoparticles of palladium or silver), batch experiments were performed and, as a suitable result, bare copper foam and copper foam coated with PdNPs were selected for the reduction column tests. Copper foam coated with PdNPs resulted in a significant increase in reduction efficiency (up to %100). In both cases, variables such as pH value, flow rate, discharge, and initial concentration of Cr(VI) were traced. The results showed that the flow rate is the most effective parameter. The presence of nitrate ions and TDS was examined, and the results reveal that increasing the nitrate concentration may result in a decrease in reduction efficiency (up to 20%), and TDS indicated no adverse effect on the reduction efficiency. Overall, the applied reduction system is practical since its efficiency is high, thereby reducing the groundwater Cr(VI) concentration below the maximum contaminant level.

ACKNOWLEDGEMENTS

This work was supported by the grant provided by the School of Environment, College of Engineering, University of Tehran, Tehran, Iran.

SUPPORTING INFORMATION

Additional information as noted in the text. This information is available via the Internet at http://www.springer.com/chemistry/journal/11814.

REFERENCES

1. WEF, *The Global Risks Report 2022*, World Economic Forum (2022).
2. C. F. Carolin, P. S. Kumar, A. Saravanan, G. J. Joshiba and M. Nau-

shad, *J. Environ. Chem. Eng.*, **5**, 2782 (2017).
3. A. Jawed, V. Saxena and L. M. Pandey, *J. Water Process Eng.*, **33**, 101009 (2020).
4. USEPA, *Chromium in Drinking Water* (2022).
5. J. Regan, N. Dushaj and G. Stinch, *ACS OMEGA* 11554 (2019).
6. Z. Ye, X. Yin, L. Chen, X. He, Z. Lin, C. Liu, S. Ning, X. Wang and Y. Wei, *J. Clean. Prod.*, **236**, 117631 (2019).
7. N. Liu, Y. Zhang, C. Xu, P. Liu, J. Lv, Y. Liu and Q. Wang, *J. Hazard. Mater.*, **384**, 121371 (2020).
8. Z. H. Farooqi, M. W. Akram, R. Begum, W. Wu and A. Irfan, *J. Hazard. Mater.*, **402**, 123535 (2020).
9. P. Liu, X. Wang, J. Ma, H. Liu and P. Ning, *Chemosphere*, **220**, 1003 (2019).
10. WHO, *Guidelines for drinking-water quality*, World Health Organization (2022).
11. J. C. Almeida, C. E. D. Cardoso, D. S. Tavares, R. Freitas, T. Trindade, C. Vale and E. Pereira, *TrAC - Trends Anal. Chem.*, **118**, 277 (2019).
12. K. Simeonidis, E. Kaprara, T. Samaras, M. Angelakeris, N. Pliatsikas, G. Vourlias, M. Mitrakas and N. Andritsos, *Sci. Total Environ.*, **535**, 61 (2015).
13. A. Addala, M. Boudiaf, M. Elektorowicz, E. Bentouhami and Y. Bengeurba, *Water Sci Technol.*, **84**, 1206 (2021).
14. L. Zhang, W. Niu, J. Sun and Q. Zhou, *Chemosphere*, **248**, 126102 (2020).
15. A. K. Mallik, A. Moktadir, A. Rahman and M. Mizanur, *J. Hazard. Mater.*, **423**, 127041 (2022).
16. S. Jamshidifard, S. Koushkbaghi, S. Hosseini, S. Rezaei, A. Karamipour, A. Jafari rad and M. Irani, *J. Hazard. Mater.*, **368**, 10 (2019).
17. V. Kumar and S. K. Dwivedi, *J. Clean. Prod.*, **295**, 126229 (2021).
18. X. Yang, Z. Zhao, G. Zhang, S. Hirayama, B. Van Nguyen, Z. Lei, K. Shimizu and Z. Zhang, *J. Hazard. Mater.*, **414**, 125479 (2021).
19. C. Su, S. Wang, Z. Zhou, H. Wang, X. Xie, Y. Yang, Y. Feng, W. Liu and P. Liu, *Sci. Total Environ.*, **768**, 144604 (2021).
20. F. Yao, M. Jia, Q. Yang, K. Luo, F. Chen, Y. Zhong, L. He, Z. Pi, K. Hou, D. Wang and X. Li, *Chemosphere*, **260**, 127537 (2020).
21. C. Barrera-Díaz, V. Lugo-Lugo, G. Roa-Morales, R. Natividad and S. A. Martínez-Delgadillo, *J. Hazard. Mater.*, **185**, 1362 (2011).
22. P. Kuang, C. Feng, M. Li, N. Chen, Q. Hu, G. Wang and R. Li, *J. Electrochem. Soc.*, **164**, E103 (2017).
23. W. Huang, M. Li, B. Zhang, C. Feng, X. Lei and B. Xu, *Water Environ. Res.*, **85**, 224 (2013).
24. M. G. Dipen Kumar Rajak, *An insight into metal based foams: processing, properties and applications*, Springer Singapore (2020).
25. L. Rajic, N. Fallahpour, E. Podlaha and A. Alshawabkeh, *Chemosphere*, **147**, 98 (2016).
26. C.-C. Ho, J.-S. Yu, S.-W. Yang, V. Ya, H. A. Le, L.-P. Cheng, K.-H. Choo and C.-W. Li, *J. Water Process Eng.*, **42**, 102191 (2021).
27. W. Jin, H. Du, S. Zheng and Y. Zhang, *Electrochim. Acta*, **191**, 1044 (2016).
28. K. Govindan, M. Noel and R. Mohan, *J. Water Process Eng.*, **6**, 58 (2015).
29. L. Rajic, N. Fallahpour, E. Podlaha and A. Alshawabkeh, *Chemosphere*, **147**, 98 (2016).
30. R. Mao, X. Zhao, H. Lan, H. Liu and J. Qu, *Water Res.*, **77**, 1 (2015).
31. W. Yang, S. Yang, W. Sun, G. Sun and Q. Xin, *J. Power Sources*, **160**, 1420 (2006).
32. S. Bajpai, S. K. Gupta, A. Dey, M. K. Jha, V. Bajpai, S. Joshi and A. Gupta, *J. Hazard. Mater.*, **227-228**, 436 (2012).
33. T. Mitra, B. Singha, N. Bar and S. K. Das, *J. Hazard. Mater.*, **273**, 94 (2014).
34. J. Li, H. Wang, L. Wang, C. Ma, C. Luan, B. Zhao, Z. Zhang, H. Zhang, X. Cheng and J. Liu, *Catalysts*, **8**, 378 (2018).
35. S. Tabatabaei, B. Forouzesh Rad and M. Baghdadi, *Chemosphere*, **251**, 126309 (2020).
36. M. Jain, V. K. Garg and K. Kadirvelu, *Bioresour. Technol.*, **102**, 600 (2011).
37. S. Mandal, S. S. Mahapatra and R. K. Patel, *J. Environ. Chem. Eng.*, **3**, 870 (2015).
38. A. Li, X. Zhao, Y. Hou, H. Liu, L. Wu and J. Qu, *Appl. Catal. B Environ.*, **111-112**, 628 (2012).